

Molecular Ω_{cc} , Ω_{bb} and Ω_{bc} states

W. F. Wang,^{1,2,*} A. Feijoo,^{2,†} J. Song,^{3,4,2,‡} and E. Oset^{2,§}

¹*Institute of Theoretical Physics, Shanxi University, Taiyuan, Shanxi 030006, China*

²*Departamento de Física Teórica and IFIC, Centro Mixto Universidad de Valencia-CSIC*

Institutos de Investigación de Paterna, Aptdo. 22085, 46071 Valencia, Spain

³*School of space and environment, Beihang University, Beijing, 102206, China*

⁴*School of Physics, Beihang University, Beijing, 102206, China*

(■Dated: December 13, 2022)

We study the interaction of meson-baryon coupled channels carrying quantum numbers of Ω_{cc} , Ω_{bb} and Ω_{bc} presently under investigation by the LHCb collaboration. The interaction is obtained from an extension of the local hidden gauge approach to the heavy quark sector that has proved to provide accurate results compared to experiment in the case of Ω_c , Ξ_c states and pentaquarks, P_c and P_{cs} . We obtain many bound states, with small decay widths within the space of the chosen coupled channels. The spin-parity of the states are $J^P = \frac{1}{2}^-$ for coupled channels of pseudoscalar-baryon ($\frac{1}{2}^+$), $J^P = \frac{3}{2}^-$ for the case of pseudoscalar-baryon ($\frac{3}{2}^+$), $J^P = \frac{1}{2}^-, \frac{3}{2}^-$ for the case of vector-baryon ($\frac{1}{2}^+$) and $J^P = \frac{1}{2}^-, \frac{3}{2}^-, \frac{5}{2}^-$ for the vector-baryon ($\frac{3}{2}^+$) channels. We look for poles of the states and evaluate the couplings to the different channels. The couplings obtained for the open channels can serve as a guide to see in which reaction the obtained states are more likely to be observed.

I. INTRODUCTION

The combined efforts in present hadron facilities are giving rise to the discovery of many new states with heavy quarks, some of them manifestly exotic, which do not follow the standard rules in terms of quarks of $q\bar{q}$ for mesons and qqq for baryons. In particular, observations of baryons Λ_c [1–5], Σ_c [6], Ξ_c [7–13], Ω_c [14], Λ_b [15–19], Σ_b [20], Ξ_b [21–24], Ω_b [25] have been reported (see Ref. [26] for a recent review of experimental findings). The discovery of the hidden charm P_c pentaquarks [27–29] and hidden charm with strangeness P_{cs} [30] has added extra excitement to the field. The search for new states continues, and motivated by the LHCb plans to measure new states, we concentrate here in the theoretical study of the Ω_{cc} , Ω_{bb} and Ω_{bc} which are presently under investigation by the LHCb collaboration¹. We should note that some attempts to search for Ω_{bc} and Ξ_{bc} have already been conducted, so far with inconclusive results [31].

These states have been the subject of intense investigation in the past using quark models [32–50]. They have also been studied in the framework of QCD lattice [42, 51–56] and the framework of QCD sum rules [57–59]. Also, different approaches have been followed in [60–63].

Our aim is to study the states of this type that can be formed as molecular states from the interaction in s-wave of mesons with baryons in their ground state. Hence, one anticipates that we shall only obtain baryon states with negative parity, different to most of the states obtained from quark models. The attractive force between mesons and baryons in many cases makes the appearance of these states unavoidable, as has been discussed in detail in [64, 65]. Also, the proximity of the mass of some states to the threshold of some meson baryon channel introduces constraints that require the explicit consideration of these channels and their interaction in a study of the baryon spectrum [66].

The work in the molecular field of meson-baryon interaction is vast and is reviewed in [67, 68]. Concerning baryons that contain heavy quarks, work has been done by different groups. The information of chiral Lagrangians is extrapolated to the charm sector to study the $\Lambda_c(2595)$ using the DN and $\Sigma_c\pi$ coupled channels in [69–72]. The molecular Ω_c states were studied in [69, 73–75]. A similar approach was used in [76], differing in the use of baryon wave functions, which were borrowed from [36] and made unnecessary to invoke elements of $SU(4)$ symmetry used in former works. The work of [76] uses an extrapolation to the charm sector of the local hidden gauge approach of [77–81] and was successful to reproduce three of the Ω_c states reported in [14]. The successful scheme, exchanging vector mesons, has then been used to make predictions for several types of baryonic states containing open charm or bottom. In this sense in [82] the Ξ_{cc} states have been studied, in [83] that work is extended to study Ξ_{bb} and Ω_{bbb} states, in [84] to study the Ξ_c and Ξ_b states, in [85] to study the Ξ_{bc} states and in [86] to study Ω_b states. Some of these states can be associated to experimental states recently found [26] and in the case of Ω_b it is

*Electronic address: wfwang@ific.uv.es

†Electronic address: edfeijoo@ific.uv.es

‡Electronic address: song-jing@buaa.edu.cn

§Corresponding author; Electronic address: oset@ific.uv.es

¹ M. Pappagallo in a talk at the SNP School 2021, <http://lambda.phys.tohoku.ac.jp/snpsc2021/>

shown in [87] that the states predicted in [86] could have already been observed in the experiment of Ref. [25] in the higher part of the spectrum. Each of the cases requires an elaborate study of the interaction with many coupled channels.

Other works also look at these states from the molecular point of view using different formalism and dynamics. In [88] one pion exchange and $D^{(*)}$ exchange are used as a source of the dynamics to study Ξ_{cc} states. In [89], heavy flavor, heavy quark spin, and heavy antiquark-diquark symmetries for hadronic molecules are considered within an effective field theory framework to study pentaquarks and open bottom, baryonic states. In [90] the one boson exchange picture is used to study Ω_c states. Particular mention deserves the extended work in different sectors, light, charm and bottom of molecular states stemming from meson baryon interaction in coupled channels using $SU(6)_{\text{lsf}} \times SU(2)_{\text{HQSS}}$ symmetry, this is $SU(6)$ flavor-spin symmetry in the light sector and $SU(2)$ in the heavy sector respecting heavy quark spin symmetry [74, 91, 92], extrapolating dynamics from the Weinberg Tomozawa interaction. These works have the virtue of correlating many coupled channels in different sectors and make qualitative predictions for bound states and resonances in a large span of quantum numbers. Ξ_b and Ξ_c states have been recently addressed from this point of view in [93].

A large number of studies of molecular states in the charm sector have been devoted to the study of pentaquarks P_c and P_{cs} . These states have hidden charm and we are concerned about open charm and bottom, so we refrain from discussing this issue and address the readers to review papers that also serve as reviews for open heavy quark baryonic molecular states [64, 65, 68, 94–97].

II. FORMALISM

A. Coupled channels for the Ω_{cc} , Ω_{bb} and Ω_{bc} states

In the first place, we must select the coupled channels that we consider in the approach. The task is facilitated by looking at the work of Ref [74]. We choose the same coupled channels eliminating only a few that appear at too high energy compared to the bulk of them. After that, the coupled channels are separated into four blocks, $PB(\frac{1}{2}^+)$, $PB(\frac{3}{2}^+)$, $VB(\frac{1}{2}^+)$, $VB(\frac{3}{2}^+)$, where P stands for the pseudoscalar meson, V for vector meson, $B(\frac{1}{2}^+)$ for ground state baryons with $J^P = \frac{1}{2}^+$ and $B(\frac{3}{2}^+)$ for ground state baryons of $J^P = \frac{3}{2}^+$. We do not mix these channels. The interaction in each block is constructed from the exchange of vector mesons obtained from the extrapolation of the local hidden gauge approach [77–81] to the charm or bottom sector [64, 65, 76, 82–86, 98]. The mixing of the blocks requires pion exchange, or of some other pseudoscalar, but these terms are not competitive with the vector exchange terms in the determination of the masses of the obtained states. They can contribute to the widths of the states, but in cases of many coupled channels where decay to states of lower mass can proceed via vector exchange, they are again not competitive (see appendix of Ref [99]). Then the coupled channels that we consider are given below and the interaction will be considered in s-wave, which determines the J^P character of the states.

TABLE I: Threshold masses (in MeV) of different channels for Ω_{cc} .

$PB(\frac{1}{2}^+), J^P = \frac{1}{2}^-$	$\Xi_{cc}\bar{K}$ 4115	$\Omega_{cc}\eta$ 4263	$\Xi_c D$ 4338	$\Xi'_c D$ 4448
$PB(\frac{3}{2}^+), J^P = \frac{3}{2}^-$	$\Xi_{cc}^*\bar{K}$ 4168	$\Omega_{cc}^*\eta$ 4320	$\Xi_c^* D$ 4516	
$VB(\frac{1}{2}^+), J^P = \frac{1}{2}^-, \frac{3}{2}^-$	$\Xi_{cc}\bar{K}^*$ 4512	$\Omega_{cc}\omega$ 4495	$\Xi_c D^*$ 4478	$\Xi'_c D^*$ 4588
$VB(\frac{3}{2}^+), J^P = \frac{1}{2}^-, \frac{3}{2}^-, \frac{5}{2}^-$	$\Xi_{cc}^*\bar{K}^*$ 4565	$\Omega_{cc}^*\omega$ 4552	$\Xi_c^* D^*$ 4656	

We obtain spin degenerate states in some cases. The degeneracy is expected to be broken with the consideration of pseudoscalar exchange terms, but with the former considerations we expect this breaking to be small. One idea of effects expected can be seen in the splitting of the two pentaquarks states P_{c2} at 4440.3 MeV and P_{c3} at 4457.3 MeV [28] from the value of the previous experiment [27] combining the two states with a peak at 4450 MeV. These states are degenerate in $J^P = \frac{1}{2}^-, \frac{3}{2}^-$ for the predictions done in [100] mostly as a $\bar{D}^*\Sigma_c$ state, and nearly degenerate in [101] where a small admixture of channels is allowed. The splitting of the states is better obtained in works considering pion exchange terms explicitly [102–104].

TABLE II: Threshold masses (in MeV) of different channels for Ω_{bb} .

$PB(\frac{1}{2}^+), J^P = \frac{1}{2}^-$	$\Xi_{bb}\bar{K}$ 10833	$\Omega_{bb}\eta$ 10778	$\Xi_b\bar{B}$ 11076	$\Xi'_b\bar{B}$ 11214
$PB(\frac{3}{2}^+), J^P = \frac{3}{2}^-$	$\Xi_{bb}^*\bar{K}$ 10863	$\Omega_{bb}^*\eta$ 10806	$\Xi_b^*\bar{B}$ 11231	
$VB(\frac{1}{2}^+), J^P = \frac{1}{2}^-, \frac{3}{2}^-$	$\Xi_{bb}\bar{K}^*$ 11230	$\Omega_{bb}\omega$ 11010	$\Xi_b\bar{B}^*$ 11122	$\Xi'_b\bar{B}^*$ 11260
$VB(\frac{3}{2}^+), J^P = \frac{1}{2}^-, \frac{3}{2}^-, \frac{5}{2}^-$	$\Xi_{bb}^*\bar{K}^*$ 11260	$\Omega_{bb}^*\omega$ 11038	$\Xi_b^*\bar{B}^*$ 11277	

TABLE III: Threshold masses (in MeV) of different channels for Ω_{bc} .

$PB(\frac{1}{2}^+), J^P = \frac{1}{2}^-$	$\Xi_{bc}\bar{K}$ 7415	$\Omega_{bc}\eta$ 7559	$\Xi_b D$ 7667	$\Xi_c\bar{B}$ 7747
$PB(\frac{1}{2}^+), J^P = \frac{1}{2}^-$	$\Xi'_{bc}\bar{K}$ 7441	$\Omega'_{bc}\eta$ 7595	$\Xi'_b D$ 7805	$\Xi'_c\bar{B}$ 7857
$PB(\frac{3}{2}^+), J^P = \frac{3}{2}^-$	$\Xi_{bc}^*\bar{K}$ 7466	$\Omega_{bc}^*\eta$ 7614	$\Xi_b^* D$ 7822	$\Xi_c^*\bar{B}$ 7925
$VB(\frac{1}{2}^+), J^P = \frac{1}{2}^-, \frac{3}{2}^-$	$\Xi_{bc}\bar{K}^*$ 7812	$\Omega_{bc}\omega$ 7791	$\Xi_b D^*$ 7807	$\Xi_c\bar{B}^*$ 7793
$VB(\frac{1}{2}^+), J^P = \frac{1}{2}^-, \frac{3}{2}^-$	$\Xi'_{bc}\bar{K}^*$ 7838	$\Omega'_{bc}\omega$ 7827	$\Xi'_b D^*$ 7945	$\Xi'_c\bar{B}^*$ 7903
$VB(\frac{3}{2}^+), J^P = \frac{1}{2}^-, \frac{3}{2}^-, \frac{5}{2}^-$	$\Xi_{bc}^*\bar{K}^*$ 7863	$\Omega_{bc}^*\omega$ 7846	$\Xi_b^* D^*$ 7962	$\Xi_c^*\bar{B}^*$ 7971

B. Baryon wave functions

The flavor of the pseudoscalar or vector mesons is trivial as they are $q_i\bar{q}_j$ states, with $q_i = u, d, s, c, b$ quarks. The baryon states require more care. We follow the procedure of Ref. [36] and single out the heaviest quark, then the symmetry or antisymmetry is imposed on the two lighter quarks, and the spin wave function is then chosen accordingly to have the wave function symmetric in spin-flavor for this couple of quarks, the color implementing the antisymmetry of the wave function. In Table IV we show explicitly the wave functions of flavor and spin taken for all the baryon states needed in our work, and where the spin wave functions within are defined, for the particular case $S_z = +1/2$, as:

$$\begin{aligned}
\chi_{MS}(12) &= \frac{1}{\sqrt{6}}(\uparrow\downarrow\uparrow + \downarrow\uparrow\uparrow - 2\uparrow\uparrow\downarrow) \\
\chi_{MS}(23) &= \frac{1}{\sqrt{6}}(\uparrow\downarrow\uparrow + \uparrow\uparrow\downarrow - 2\downarrow\uparrow\uparrow) \\
\chi_{MA}(23) &= \frac{1}{\sqrt{2}}(\uparrow\uparrow\downarrow - \uparrow\downarrow\uparrow).
\end{aligned} \tag{1}$$

TABLE IV: Wave functions of baryon states.

State	I, J	flavor	spin
Ξ_{cc}^{++}	1/2, 1/2	ccu	$\chi_{MS}(12)$
Ξ_{cc}^+	1/2, 1/2	ccd	$\chi_{MS}(12)$
Ω_{cc}^+	0, 1/2	ccs	$\chi_{MS}(12)$
Ξ_c^+	1/2, 1/2	$\frac{1}{\sqrt{2}}c(us - su)$	$\chi_{MA}(23)$
Ξ_c^0	1/2, 1/2	$\frac{1}{\sqrt{2}}c(ds - sd)$	$\chi_{MA}(23)$
$\Xi_c'^+$	1/2, 1/2	$\frac{1}{\sqrt{2}}c(us + su)$	$\chi_{MS}(23)$
$\Xi_c'^0$	1/2, 1/2	$\frac{1}{\sqrt{2}}c(ds + sd)$	$\chi_{MS}(23)$
Ω_c^0	0, 1/2	css	$\chi_{MS}(23)$
Ξ_{bb}^0	1/2, 1/2	bbu	$\chi_{MS}(12)$
Ξ_{bb}^-	1/2, 1/2	bbd	$\chi_{MS}(12)$
Ω_{bb}^-	0, 1/2	bbs	$\chi_{MS}(12)$
Ξ_b^0	1/2, 1/2	$\frac{1}{\sqrt{2}}b(us - su)$	$\chi_{MA}(23)$
Ξ_b^-	1/2, 1/2	$\frac{1}{\sqrt{2}}b(ds - sd)$	$\chi_{MA}(23)$
$\Xi_b'^0$	1/2, 1/2	$\frac{1}{\sqrt{2}}b(us + su)$	$\chi_{MS}(23)$
$\Xi_b'^-$	1/2, 1/2	$\frac{1}{\sqrt{2}}b(ds + sd)$	$\chi_{MS}(23)$
Ω_b^-	0, 1/2	bss	$\chi_{MS}(23)$
Ω_{bc}^0	0, 1/2	$\frac{1}{\sqrt{2}}b(cs - sc)$	$\chi_{MA}(23)$
$\Omega_{bc}'^0$	0, 1/2	$\frac{1}{\sqrt{2}}b(cs + sc)$	$\chi_{MS}(23)$
Ξ_{bc}^+	1/2, 1/2	$\frac{1}{\sqrt{2}}b(cu - uc)$	$\chi_{MA}(23)$
$\Xi_{bc}'^+$	1/2, 1/2	$\frac{1}{\sqrt{2}}b(cu + uc)$	$\chi_{MS}(23)$
Ξ_{bc}^0	1/2, 1/2	$\frac{1}{\sqrt{2}}b(cd - dc)$	$\chi_{MA}(23)$
$\Xi_{bc}'^0$	1/2, 1/2	$\frac{1}{\sqrt{2}}b(cd + dc)$	$\chi_{MS}(23)$
Ξ_{cc}^{*++}	1/2, 3/2	ccu	χ_S
Ξ_{cc}^{*+}	1/2, 3/2	ccd	χ_S
Ω_{cc}^{*+}	0, 3/2	ccs	χ_S
Ξ_c^{*+}	1/2, 3/2	$\frac{1}{\sqrt{2}}c(us + su)$	χ_S
Ξ_c^{*0}	1/2, 3/2	$\frac{1}{\sqrt{2}}c(ds + sd)$	χ_S
Ω_c^{*0}	0, 3/2	css	χ_S
Ξ_{bb}^{*0}	1/2, 3/2	bbu	χ_S
Ξ_{bb}^{*-}	1/2, 3/2	bbd	χ_S
Ω_{bb}^{*-}	0, 3/2	bbs	χ_S
Ξ_b^{*0}	1/2, 3/2	$\frac{1}{\sqrt{2}}b(us + su)$	χ_S
Ξ_b^{*-}	1/2, 3/2	$\frac{1}{\sqrt{2}}b(ds + sd)$	χ_S
Ω_b^{*-}	0, 3/2	bss	χ_S
Ξ_{bc}^{*+}	1/2, 3/2	$\frac{1}{\sqrt{2}}b(cu + uc)$	χ_S
Ξ_{bc}^{*0}	1/2, 3/2	$\frac{1}{\sqrt{2}}b(cd + dc)$	χ_S
Ω_{bc}^{*0}	0, 3/2	$\frac{1}{\sqrt{2}}b(cs + sc)$	χ_S

We also must consider the isospin combinations of the states. For this we need to express our phase convention $\left\{ \begin{matrix} \bar{K}^0 \\ -K^- \end{matrix} \right\}, \left\{ \begin{matrix} D^+ \\ -D^0 \end{matrix} \right\}, \left\{ \begin{matrix} \bar{B}^0 \\ -B^- \end{matrix} \right\}, \left\{ \begin{matrix} \Xi_c^+ \\ \Xi_c^0 \end{matrix} \right\}, \left\{ \begin{matrix} \Xi_b^0 \\ \Xi_b^- \end{matrix} \right\}, \left\{ \begin{matrix} \Xi_{cc}^{++} \\ \Xi_{cc}^+ \end{matrix} \right\}, \left\{ \begin{matrix} \Xi_{bb}^0 \\ \Xi_{bb}^- \end{matrix} \right\}, \left\{ \begin{matrix} \Xi_{bc}^+ \\ \Xi_{bc}^0 \end{matrix} \right\}$, and then the isospin wave functions are given by:

$$\begin{aligned}
|\Xi_{cc}^{(*)}\bar{K}^{(*)}, I=0\rangle &= -\frac{1}{\sqrt{2}}(|\Xi_{cc}^{(*)++}K^{(*)-}\rangle + |\Xi_{cc}^{(*)+}\bar{K}^{(*)0}\rangle) \\
|\Omega_{cc}^{(*)}\eta, I=0\rangle &= |\Omega_{cc}^{(*)+}\eta\rangle \\
|\Omega_{cc}^{(*)}\omega, I=0\rangle &= |\Omega_{cc}^{(*)+}\omega\rangle
\end{aligned} \tag{2}$$

$$\begin{aligned}
|\Xi_c^{(*)} D^{(*)}, I=0\rangle &= -\frac{1}{\sqrt{2}}(|\Xi_c^{(*)+} D^{(*)0}\rangle + |\Xi_c^{(*)0} D^{(*)+}\rangle) \\
|\Xi_c' D^{(*)}, I=0\rangle &= -\frac{1}{\sqrt{2}}(|\Xi_c'^+ D^{(*)0}\rangle + |\Xi_c'^0 D^{(*)+}\rangle) \\
|\Xi_{bb}^{(*)} \bar{K}^{(*)}, I=0\rangle &= -\frac{1}{\sqrt{2}}(|\Xi_{bb}^{(*)0} K^{(*)-}\rangle + |\Xi_{bb}^{(*)-} \bar{K}^{(*)0}\rangle) \\
|\Omega_{bb}^{(*)} \eta, I=0\rangle &= |\Omega_{bb}^{(*)-} \eta\rangle \\
|\Omega_{bb}^{(*)} \omega, I=0\rangle &= |\Omega_{bb}^{(*)-} \omega\rangle \\
|\Xi_b^{(*)} \bar{B}^{(*)}, I=0\rangle &= -\frac{1}{\sqrt{2}}(|\Xi_b^{(*)0} B^{(*)-}\rangle + |\Xi_b^{(*)-} \bar{B}^{(*)0}\rangle) \\
|\Xi_b' \bar{B}^{(*)}, I=0\rangle &= -\frac{1}{\sqrt{2}}(|\Xi_b'^0 B^{(*)-}\rangle + |\Xi_b'^- \bar{B}^{(*)0}\rangle) \\
|\Xi_{bc}^{(*)} \bar{K}^{(*)}, I=0\rangle &= -\frac{1}{\sqrt{2}}(|\Xi_{bc}^{(*)+} K^{(*)-}\rangle + |\Xi_{bc}^{(*)0} \bar{K}^{(*)0}\rangle) \\
|\Xi_{bc}' \bar{K}^{(*)}, I=0\rangle &= -\frac{1}{\sqrt{2}}(|\Xi_{bc}'^+ K^{(*)-}\rangle + |\Xi_{bc}'^0 \bar{K}^{(*)0}\rangle) \\
|\Omega_{bc}^{(*)} \eta, I=0\rangle &= |\Omega_{bc}^{(*)0} \eta\rangle \\
|\Omega_{bc}' \eta, I=0\rangle &= |\Omega_{bc}'^0 \eta\rangle \\
|\Omega_{bc}^{(*)} \omega, I=0\rangle &= |\Omega_{bc}^{(*)0} \omega\rangle \\
|\Omega_{bc}' \omega, I=0\rangle &= |\Omega_{bc}'^0 \omega\rangle \\
|\Xi_b^{(*)} D^{(*)}, I=0\rangle &= -\frac{1}{\sqrt{2}}(|\Xi_b^{(*)0} D^{(*)0}\rangle + |\Xi_b^{(*)-} D^{(*)+}\rangle) \\
|\Xi_b' D^{(*)}, I=0\rangle &= -\frac{1}{\sqrt{2}}(|\Xi_b'^0 D^{(*)0}\rangle + |\Xi_b'^- D^{(*)+}\rangle) \\
|\Xi_c^{(*)} \bar{B}^{(*)}, I=0\rangle &= -\frac{1}{\sqrt{2}}(|\Xi_c^{(*)+} B^{(*)-}\rangle + |\Xi_c^{(*)0} \bar{B}^{(*)0}\rangle) \\
|\Xi_c' \bar{B}^{(*)}, I=0\rangle &= -\frac{1}{\sqrt{2}}(|\Xi_c'^+ B^{(*)-}\rangle + |\Xi_c'^0 \bar{B}^{(*)0}\rangle).
\end{aligned}$$

C. Interaction between coupled channels

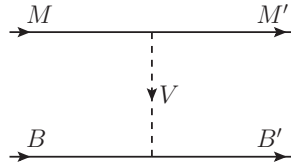


FIG. 1: Diagrammatic representation of the interaction $MB \rightarrow M'B'$ through the exchange of vector mesons. The $M(M')$ and $B(B')$ are the initial (final) meson and baryon states, respectively, while V stands for the vector meson exchanged.

As mentioned above, we use vector exchange from the extension of the local hidden gauge approach between mesons and baryons as shown in the Fig. 1. The VMM' vertex has two types for our set of states, VPP ($V \equiv$ vector, $P \equiv$ pseudoscalar) and VVV , which are described by the following Lagrangians

$$\mathcal{L}_{VPP} = -ig \langle [P, \partial_\mu P] V^\mu \rangle, \quad (3)$$

$$\mathcal{L}_{VVV} = ig \langle (V^\mu \partial_\nu V_\mu - \partial_\nu V^\mu V_\mu) V^\nu \rangle. \quad (4)$$

The coupling $g = \frac{m_V}{2f_\pi}$ with $m_V = 800$ MeV and the pion decay constant $f_\pi = 93$ MeV. And the P or V above are the $q_i \bar{q}_j$ matrices written in terms of mesons and the symbol $\langle \cdot \cdot \cdot \rangle$ means the trace for the matrices. We must recall that, while $q_i \bar{q}_j$ are

SU(4) or SU(5) matrices, the vertices of Eqs. (3) and (4) only use the overlap of $q\bar{q}$ in the external mesons and the exchanged vectors, hence the use of the SU(4), SU(5) symmetry is superfluous [105].

The matrices P and V that we need are given by

$$P = \begin{pmatrix} \frac{1}{\sqrt{2}}\pi^0 + \frac{1}{\sqrt{3}}\eta + \frac{1}{\sqrt{6}}\eta' & \pi^+ & K^+ & \bar{D}^0 \\ \pi^- & -\frac{1}{\sqrt{2}}\pi^0 + \frac{1}{\sqrt{3}}\eta + \frac{1}{\sqrt{6}}\eta' & K^0 & D^- \\ K^- & \bar{K}^0 & -\frac{1}{\sqrt{3}}\eta + \sqrt{\frac{2}{3}}\eta' & D_s^- \\ D^0 & D^+ & D_s^+ & \eta_c \end{pmatrix}, \quad (5)$$

$$V = \begin{pmatrix} \frac{1}{\sqrt{2}}\rho^0 + \frac{1}{\sqrt{2}}\omega & \rho^+ & K^{*+} & \bar{D}^{*0} \\ \rho^- & -\frac{1}{\sqrt{2}}\rho^0 + \frac{1}{\sqrt{2}}\omega & K^{*0} & \bar{D}^{*-} \\ K^{*-} & \bar{K}^{*0} & \phi & D_s^{*-} \\ D^{*0} & D^{*+} & D_s^{*+} & J/\psi \end{pmatrix}, \quad (6)$$

for the mesons in the charm sector, and

$$P = \begin{pmatrix} \frac{1}{\sqrt{2}}\pi^0 + \frac{1}{\sqrt{3}}\eta + \frac{1}{\sqrt{6}}\eta' & \pi^+ & K^+ & B^+ \\ \pi^- & -\frac{1}{\sqrt{2}}\pi^0 + \frac{1}{\sqrt{3}}\eta + \frac{1}{\sqrt{6}}\eta' & K^0 & B^0 \\ K^- & \bar{K}^0 & -\frac{1}{\sqrt{3}}\eta + \sqrt{\frac{2}{3}}\eta' & B_s^0 \\ B^- & \bar{B}^0 & \bar{B}_s^0 & \eta_b \end{pmatrix}, \quad (7)$$

$$V = \begin{pmatrix} \frac{1}{\sqrt{2}}\rho^0 + \frac{1}{\sqrt{2}}\omega & \rho^+ & K^{*+} & B^{*+} \\ \rho^- & -\frac{1}{\sqrt{2}}\rho^0 + \frac{1}{\sqrt{2}}\omega & K^{*0} & B^{*0} \\ K^{*-} & \bar{K}^{*0} & \phi & B_s^{*0} \\ B^{*-} & \bar{B}^{*0} & \bar{B}_s^{*0} & \Upsilon \end{pmatrix}, \quad (8)$$

for the bottom sector.

We also note that we evaluate the VVV interaction assuming that the external three momenta are small versus the vector mass and then can be neglected. In this case the vector V^ν in Eq. (4) cannot be the external vector since $\epsilon^0 = 0$ for the vector at rest, the ν are spatial components and ∂_ν will give three vectors which are null. Then V^ν corresponds to the exchanged vector. Eq. (4) is then equivalent to Eq. (3) substituting the P of a given $q\bar{q}$ by the corresponding V and adding the $-\epsilon^\mu\epsilon'_\mu = \vec{\epsilon} \cdot \vec{\epsilon}'$ factor for the polarization of the two external vectors.

The lower vertex of Fig. 1 is rendered easy to evaluate using the wave functions of Table IV. Rather than using effective Lagrangians in terms of the mesons and baryons which require extension of chiral Lagrangians from SU(3) to SU(4) or SU(5) [69, 70, 75], we write the operator in terms of quarks and sandwich it with the baryon wave functions of Table IV [76]. The vertex is given by

$$\tilde{\mathcal{L}}_{VBB} \equiv gq\bar{q}(V), \quad (9)$$

where $q\bar{q}(V)$ is the vector wave function in terms of quarks, hence

$$\tilde{\mathcal{L}}_{VBB} \equiv g \begin{pmatrix} \frac{1}{\sqrt{2}}(u\bar{u} - d\bar{d}), & \rho^0 \\ \frac{1}{\sqrt{2}}(u\bar{u} + d\bar{d}), & \omega \\ s\bar{s}, & \phi \end{pmatrix}, \quad (10)$$

in the neutral light vector exchange. It is worth mentioning that the exchange of light vector mesons obtained using SU(4) symmetry in [69, 70, 75] coincides with the formalism of [76] since the heavy quarks are spectators and only the light quarks play a role, hence one is not making use of SU(4) symmetry, but only of its SU(3) subgroup. Since the exchange of light vector mesons provide the dominant contribution, it is not surprising to see that the results of [75] and [76] are very similar. The other point worth mentioning is that for these dominant terms, since the heavy quarks are spectators, the interaction does not depend upon them and then the heavy quark symmetries [106] are automatically fulfilled.

An example of how the $MB \rightarrow M'B'$ potential is obtained combining the two vertices of Fig. 1 and the vector propagator is shown in the Appendix of Ref. [76]. It is very easy and we refrain from repeating it here.

The evaluation of the transition potential V_{ij} from one channel to another in the blocks we have selected is then straightforward, but we can simplify the calculation with the following observation [83]. Since the VBB vertex is spin independent we classify the state in blocks that have $\chi_{MS}(23)$, $\chi_{MA}(23)$ and χ_S . Since $\chi_{MS}(12)$ have overlap with $\chi_{MS}(23)$ and $\chi_{MA}(23)$, we must keep the states of $\chi_{MS}(12)$ in the blocks of $\chi_{MS}(23)$ and $\chi_{MA}(23)$. The overlap of these spin functions are given by

$$\langle \chi_{MS}(12) | \chi_{MS}(23) \rangle = -\frac{1}{2}, \quad (11)$$

$$\langle \chi_{MS}(12) | \chi_{MA}(23) \rangle = -\frac{\sqrt{3}}{2}. \quad (12)$$

However, even if the $\Xi'_c D$ and $\Xi_c D$ states do not mix in the calculation of the potential, in the T matrix they will mix through the intermediate $\Xi_{cc} \bar{K}$ and $\Omega_{cc} \eta$ states. Hence, we write the matrix V_{ij} for all the states of PB . This said, we have the following blocks.

D. Spin blocks for Ω_{cc} state

- i) $PB(\frac{1}{2}^+)$ channels: $\Xi_{cc} \bar{K}$, $\Omega_{cc} \eta$, $\Xi_c D$, and $\Xi'_c D$.
- ii) $PB(\frac{3}{2}^+)$ channels: $\Xi_{cc}^* \bar{K}$, $\Omega_{cc}^* \eta$, $\Xi_c^* D$
- iii) $VB(\frac{1}{2}^+)$ channels: $\Xi_{cc} \bar{K}^*$, $\Xi_c D^*$, $\Omega_{cc} \omega$, and $\Xi'_c D^*$.
- iv) $VB(\frac{3}{2}^+)$ channels: $\Xi_{cc}^* \bar{K}^*$, $\Omega_{cc}^* \omega$, $\Xi_c^* D^*$.

The interaction obtained for the mechanism of Fig. 1 is always of the type

$$V_{ij} = -\frac{1}{4f_\pi^2} (p_1^0 + p_3^0) C_{ij}, \quad (13)$$

where p_1^0 , p_3^0 are the energies of the initial and final mesons, respectively. The coefficient C_{ij} are then evaluated and we find the following Tables V-VIII for the blocks described before. The λ below is a suppression factor of the order $m_V^2/m_{D^*}^2$ coming from the exchange of a D^* rather than a light vector. Following Ref. [76] we take the value $\lambda = 0.25$ in the numerical calculations.

TABLE V: Coefficients C_{ij} for the PB sector with $J^P = \frac{1}{2}^-$.

	$\Xi_{cc} \bar{K}$	$\Omega_{cc} \eta$	$\Xi_c D$	$\Xi'_c D$
$\Xi_{cc} \bar{K}$	2	$\frac{2\sqrt{2}}{\sqrt{3}}$	$\frac{-\sqrt{3}}{2\sqrt{2}} \lambda$	$\frac{1}{2\sqrt{2}} \lambda$
$\Omega_{cc} \eta$		0	$-\frac{1}{2} \lambda$	$\frac{-1}{2\sqrt{3}} \lambda$
$\Xi_c D$			2	0
$\Xi'_c D$				2

TABLE VI: Coefficients C_{ij} for the VB sector with $J^P = \frac{1}{2}^-, \frac{3}{2}^-$.

	$\Xi_c D^*$	$\Omega_{cc} \omega$	$\Xi_{cc} \bar{K}^*$	$\Xi'_c D^*$
$\Xi_c D^*$	2	$\frac{-\sqrt{3}}{2\sqrt{2}} \lambda$	$\frac{-\sqrt{3}}{2\sqrt{2}} \lambda$	0
$\Omega_{cc} \omega$		0	1	$\frac{-1}{2\sqrt{2}} \lambda$
$\Xi_{cc} \bar{K}^*$			2	$\frac{1}{2\sqrt{2}} \lambda$
$\Xi'_c D^*$				2

TABLE VII: Coefficients C_{ij} for the PB sector with $J^P = \frac{3}{2}^-$.

	$\Xi_{cc}^* \bar{K}$	$\Omega_{cc}^* \eta$	$\Xi_c^* D$
$\Xi_{cc}^* \bar{K}$	2	$\frac{2\sqrt{2}}{\sqrt{3}}$	$\frac{1}{\sqrt{2}}\lambda$
$\Omega_{cc}^* \eta$		0	$\frac{1}{\sqrt{3}}\lambda$
$\Xi_c^* D$			2

TABLE VIII: Coefficients C_{ij} for the VB sector with $J^P = \frac{1}{2}^-, \frac{3}{2}^-, \frac{5}{2}^-$.

	$\Omega_{cc}^* \omega$	$\Xi_{cc}^* \bar{K}^*$	$\Xi_c^* D^*$
$\Omega_{cc}^* \omega$	0	1	$\frac{1}{\sqrt{2}}\lambda$
$\Xi_{cc}^* \bar{K}^*$		2	$\frac{1}{\sqrt{2}}\lambda$
$\Xi_c^* D^*$			2

E. Spin blocks for Ω_{bb} states

In these sectors we have taken zero the terms that go with the exchange of B^* , since $m_V^2/m_{B^*}^2$ is negligible. We follow the same steps as before and find the C_{ij} coefficients and the channels belonging to each block as shown in Tables IX-XII.

TABLE IX: Coefficients C_{ij} for the PB sector with $J^P = \frac{1}{2}^-$.

	$\Omega_{bb}\eta$	$\Xi_{bb}\bar{K}$	$\Xi_b\bar{B}$	$\Xi'_b\bar{B}$
$\Omega_{bb}\eta$	0	$\frac{2\sqrt{2}}{\sqrt{3}}$	0	0
$\Xi_{bb}\bar{K}$		2	0	0
$\Xi_b\bar{B}$			2	0
$\Xi'_b\bar{B}$				2

TABLE X: Coefficients C_{ij} for the VB sector with $J^P = \frac{1}{2}^-, \frac{3}{2}^-$.

	$\Omega_{bb}\omega$	$\Xi_b\bar{B}^*$	$\Xi_{bb}\bar{K}^*$	$\Xi'_b\bar{B}^*$
$\Omega_{bb}\omega$	0	0	1	0
$\Xi_b\bar{B}^*$		2	0	0
$\Xi_{bb}\bar{K}^*$			2	0
$\Xi'_b\bar{B}^*$				2

TABLE XI: Coefficients C_{ij} for the PB sector with $J^P = \frac{3}{2}^-$.

	$\Omega_{bb}^* \eta$	$\Xi_{bb}^* \bar{K}$	$\Xi_b^* \bar{B}$
$\Omega_{bb}^* \eta$	0	$\frac{2\sqrt{2}}{\sqrt{3}}$	0
$\Xi_{bb}^* \bar{K}$		2	0
$\Xi_b^* \bar{B}$			2

TABLE XII: Coefficients C_{ij} for the VB sector with $J^P = \frac{1}{2}^-, \frac{3}{2}^-, \frac{5}{2}^-$.

	$\Omega_{bb}^*\omega$	$\Xi_{bb}^*\bar{K}^*$	$\Xi_b^*\bar{B}^*$
$\Omega_{bb}^*\omega$	0	1	0
$\Xi_{bb}^*\bar{K}^*$		2	0
$\Xi_b^*\bar{B}^*$			2

F. Spin blocks of Ω_{bc}

The C_{ij} coefficients and the channels belonging to each block are shown in Tables XIII-XVI.

TABLE XIII: Coefficients C_{ij} for the PB sector with $J^P = \frac{1}{2}^-$.

	$\Xi_{bc}\bar{K}$	$\Xi'_{bc}\bar{K}$	$\Omega_{bc}\eta$	$\Omega'_{bc}\eta$	$\Xi_b D$	$\Xi_c\bar{B}$	$\Xi'_b D$	$\Xi'_c\bar{B}$
$\Xi_{bc}\bar{K}$	2	0	$\frac{2\sqrt{2}}{\sqrt{3}}$	0	λ	0	0	0
$\Xi'_{bc}\bar{K}$		2	0	$\frac{2\sqrt{2}}{\sqrt{3}}$	0	0	$-\lambda$	0
$\Omega_{bc}\eta$			0	0	$\frac{\sqrt{2}}{\sqrt{3}}\lambda$	0	0	0
$\Omega'_{bc}\eta$				0	0	0	$\frac{\sqrt{2}}{\sqrt{3}}\lambda$	0
$\Xi_b D$					2	0	0	0
$\Xi_c\bar{B}$						2	0	0
$\Xi'_b D$							2	0
$\Xi'_c\bar{B}$								2

TABLE XIV: Coefficients C_{ij} for the VB sector with $J^P = \frac{1}{2}^-, \frac{3}{2}^-$.

	$\Omega_{bc}\omega$	$\Xi_c\bar{B}^*$	$\Xi_b D^*$	$\Xi_{bc}\bar{K}^*$	$\Omega'_{bc}\omega$	$\Xi'_{bc}\bar{K}^*$	$\Xi'_c\bar{B}^*$	$\Xi'_b D^*$
$\Omega_{bc}\omega$	0	0	λ	1	0	0	0	0
$\Xi_c\bar{B}^*$		2	0	0	0	0	0	0
$\Xi_b D^*$			2	λ	0	0	0	0
$\Xi_{bc}\bar{K}^*$				2	0	0	0	0
$\Omega'_{bc}\omega$					0	1	0	λ
$\Xi'_{bc}\bar{K}^*$						2	0	$-\lambda$
$\Xi'_c\bar{B}^*$							2	0
$\Xi'_b D^*$								2

TABLE XV: Coefficients C_{ij} for the PB sector with $J^P = \frac{3}{2}^-$.

	$\Xi_{bc}^*\bar{K}$	$\Omega_{bc}^*\eta$	$\Xi_b^* D$	$\Xi_c^*\bar{B}$
$\Xi_{bc}^*\bar{K}$	2	$\frac{2\sqrt{2}}{\sqrt{3}}$	λ	0
$\Omega_{bc}^*\eta$		0	$\frac{\sqrt{2}}{\sqrt{3}}\lambda$	0
$\Xi_b^* D$			2	0
$\Xi_c^*\bar{B}$				2

TABLE XVI: Coefficients C_{ij} for the VB sector with $J^P = \frac{1}{2}^-, \frac{3}{2}^-, \frac{5}{2}^-$.

	$\Omega_{bc}^*\omega$	$\Xi_{bc}^*\bar{K}^*$	$\Xi_b^*D^*$	$\Xi_c^*\bar{B}^*$
$\Omega_{bc}^*\omega$	0	1	λ	0
$\Xi_{bc}^*\bar{K}^*$		2	λ	0
$\Xi_b^*D^*$			2	0
$\Xi_c^*\bar{B}^*$				2

G. Scattering matrix and pole

Once the V_{ij} potential has been calculated, we obtain the scattering matrix in the Bethe-Salpeter equation in coupled channels

$$T = [1 - VG]^{-1}V \quad (14)$$

in the matrix form, where G is the diagonal loop function for the meson baryon intermediate state, which we take in the cutoff form as in [76] with $q_{max} = 650$ MeV.

The poles are reached in the second Riemann sheet for which we change $G \rightarrow G^{II}$ as

$$G_j^{II} = G_j^I + i\frac{2M_j q}{4\pi\sqrt{s}}, \quad (15)$$

for $\text{Re}\sqrt{s} > m_j + M_j$, and q given by

$$q = \frac{\lambda^{1/2}(s, m_j^2, M_j^2)}{2\sqrt{s}}, \quad (16)$$

with m_j and M_j the masses of the meson and baryon, respectively. We also evaluate the couplings defined from the residue at the pole where the amplitudes go as

$$T_{ij} = \frac{g_i g_j}{z - z_R}, \quad (17)$$

with z_R the complex energy ($M, i\Gamma/2$). We choose one sign for one g_i and the rest of the couplings have the relative sign well defined. We also show $g_i G_i^{II}$, which gives the wave function at the origin in coordinate space [107].

III. RESULTS

In the first place we write in Table XVII, the masses of the mesons and baryons which are needed for the calculations. Those not in the PDG [108] are taken from [109]. For further discussion about the energies obtained, we also show the masses of the thresholds of the different channels in Table I.

TABLE XVII: Masses of mesons and baryons in the units of MeV, the values not in the PDG [108] are taken from [109].

States	\bar{K}	η	D	\bar{B}	ω	\bar{K}^*	D^*
Masses	493	548	1870	5279	780	890	2010
States	\bar{B}^*	Ξ_c	Ξ_c'	Ξ_c^*	Ξ_b	Ξ_b'	Ξ_b^*
Masses	5325	2468	2578	2646	5797	5935	5952
States	Ξ_{cc}	Ξ_{cc}^*	Ξ_{bb}	Ξ_{bb}^*	Ξ_{bc}	Ξ_{bc}'	Ξ_{bc}^*
Masses	3622	3675	10340	10370	6922	6948	6973
States	Ω_{cc}	Ω_{cc}^*	Ω_{bb}	Ω_{bb}^*	Ω_{bc}	Ω_{bc}'	Ω_{bc}^*
Masses	3715	3772	10230	10258	7011	7047	7066

A. Poles and their coupling constants of Ω_{cc}

In Tables XVIII-XXI we write the masses of the states obtained, together with the couplings to each channel and the wave function at the origin. The calculations have been done using $q_{max} = 650$ MeV, which was found suited for the study of the Ω_c states in [76], where three experimental states could be associated with molecular states. We write in bold characters the case of the biggest coupling, and wave function at the origin, which indicates the most relevant channel.

TABLE XVIII: The poles for Ω_{cc} along with their coupling constants (in units of MeV) to various channels in the $J^P = \frac{1}{2}^-$ sector from $PB(\frac{1}{2}^+)$.

Poles		$\Xi_{cc}\bar{K}$	$\Omega_{cc}\eta$	$\Xi_c D$	$\Xi'_c D$
4069.86	g_i	2.63	1.55	-1.10	0.26
	$g_i G_i^{II}$	-40.42	-13.26	3.59	-0.65
4205.22 + $i0.94$	g_i	0.10 + $i0.20$	0.04 + $i0.09$	6.25 - $i0.04$	0.09 + $i0.01$
	$g_i G_i^{II}$	-5.86 - $i1.84$	-0.57 - $i1.32$	-31.79 + $i0.06$	-0.30 - $i0.05$
4310.76 + $i0.28$	g_i	0.02 + $i0.01$	-0.13 - $i0.04$	-0.02 + $i0.00$	6.35 + $i0.00$
	$g_i G_i^{II}$	-0.45 + $i0.64$	3.47 - $i0.96$	0.23 - $i0.01$	-31.95 - $i0.05$

TABLE XIX: The poles for Ω_{cc} along with their coupling constants (in units of MeV) to various channels in the $J^P = \frac{1}{2}^-, \frac{3}{2}^-$ sector from $VB(\frac{1}{2}^+)$.

Poles		$\Xi_c D^*$	$\Omega_{cc}\omega$	$\Xi_{cc}\bar{K}^*$	$\Xi'_c D^*$
4332.86	g_i	6.51	-0.70	-1.35	-0.07
	$g_i G_i^{II}$	-29.78	5.66	9.74	0.23
4405.47	g_i	1.27	1.41	3.81	0.83
	$g_i G_i^{II}$	-8.44	-15.17	-35.89	-3.33
4446.29	g_i	-0.08	-0.32	-0.24	6.58
	$g_i G_i^{II}$	0.73	4.34	2.81	-30.80

TABLE XX: The poles for Ω_{cc} along with their coupling constants (in units of MeV) to various channels in the $J^P = \frac{3}{2}^-$ sector from $PB(\frac{3}{2}^+)$.

Poles		$\Xi_{cc}^*\bar{K}$	$\Omega_{cc}^*\eta$	$\Xi_c^* D$
4123.85	g_i	2.62	1.55	0.84
	$g_i G_i^{II}$	-40.61	-13.14	-2.09
4380.36 + $i0.73$	g_i	-0.01 - $i0.15$	0.02 - $i0.05$	6.28 - $i0.03$
	$g_i G_i^{II}$	4.71 + $i0.76$	0.41 + $i1.37$	-31.94 + $i0.05$

TABLE XXI: The poles for Ω_{cc} along with their coupling constants (in units of MeV) to various channels in the $J^P = \frac{1}{2}^-, \frac{3}{2}^-, \frac{5}{2}^-$ sector from $VB(\frac{3}{2}^+)$.

Poles		$\Omega_{cc}^*\omega$	$\Xi_{cc}^*\bar{K}^*$	$\Xi_c^* D^*$
4446.59	g_i	1.59	3.93	2.64
	$g_i G_i^{II}$	-16.03	-35.31	-9.69
4520.38	g_i	-0.18	-0.94	6.10
	$g_i G_i^{II}$	2.78	12.44	-29.41

By looking at Table XVIII we observe that we obtain states at 4070, 4205, 4311 MeV. The widths, corresponding to twice the imaginary part at the pole, are all below 2 MeV, the most relevant channels are the $\Xi_{cc}\bar{K}$ for the 4070 MeV, the $\Xi_c D$ for the

4205 MeV and the $\Xi'_c D$ for the 4311 MeV. The $\Omega_{cc}\eta$ channel has a relatively important weight also in the 4070 MeV state, but is negligible in the other states. By looking at the thresholds in the Table I, we see that the 4070 MeV state could mostly qualify as a $\Xi_{cc}\bar{K}$ molecule with a binding of about 45 MeV, the 4311 state would be mostly a $\Xi_c D$ state bound by about 133 MeV and the 4311 would correspond to a $\Xi'_c D$ state bound by about 137 MeV. However we should not ignore that we have a mixture of coupled channels in the wave functions and some components are less bound than others, hence it is not fully appropriate to put all the binding in just one component, the total energies being the relevant magnitudes to be considered. In Table XIX we find similar features to the former one with three states that couple mostly to $\Xi_c D^*$, $\Xi_{cc}\bar{K}^*$, and $\Xi'_c D^*$ respectively.

In Table XX we obtain two states of $PB(\frac{3}{2}^+)$ nature at 4124 MeV and 4380 MeV, which couple mostly to $\Xi_{cc}^*\bar{K}$ and $\Xi_c^* D$ respectively. The widths are also smaller than 2 MeV. In Table XXI we also obtain two states of $VB(\frac{3}{2}^+)$ nature, and hence $J^P = \frac{1}{2}^-, \frac{3}{2}^-, \frac{5}{2}^-$, that couple mostly to $\Xi_{cc}^*\bar{K}^*$ and $\Xi_c^* D^*$ respectively. The widths are null with the space of states considered, hence we expect them to be very small.

B. Poles and their coupling constants of Ω_{bb}

In Table II we put the threshold of the channels involved in the calculations. In Tables XXII - XXV, we show the bound states and resonances of Ω_{bb} as well as their coupling constants to various channels, obtained with $q_{max} = 650$ MeV.

TABLE XXII: The poles for Ω_{bb} along with their coupling constants (in units of MeV) to various channels in the $J^P = \frac{1}{2}^-$ sector from $PB(\frac{1}{2}^+)$.

Poles		$\Omega_{bb}\eta$	$\Xi_{bb}\bar{K}$	$\Xi_b\bar{B}$	$\Xi'_b\bar{B}$
10741.65	g_i	1.50	2.72	0	0
	$g_i G_i^{II}$	-25.56	-34.78	0	0
10864.15	g_i	0	0	11.87	0
	$g_i G_i^{II}$	0	0	-20.43	0
11001.63	g_i	0	0	0	11.87
	$g_i G_i^{II}$	0	0	0	-20.43

TABLE XXIII: The poles for Ω_{bb} along with their coupling constants (in units of MeV) to various channels in the $J^P = \frac{1}{2}^-, \frac{3}{2}^-$ sector from $VB(\frac{1}{2}^+)$.

Poles		$\Omega_{bb}\omega$	$\Xi_b\bar{B}^*$	$\Xi_{bb}\bar{K}^*$	$\Xi'_b\bar{B}^*$
10909.88	g_i	0	11.92	0	0
	$g_i G_i^{II}$	0	-20.35	0	0
11047.36	g_i	0	0	0	11.92
	$g_i G_i^{II}$	0	0	0	-20.34

TABLE XXIV: The poles for Ω_{bb} along with their coupling constants (in units of MeV) to various channels in the $J^P = \frac{3}{2}^-$ sector from $PB(\frac{3}{2}^+)$.

Poles		$\Omega_{bb}^*\eta$	$\Xi_{bb}^*\bar{K}$	$\Xi_b^*\bar{B}$
10770.91	g_i	1.50	2.71	0
	$g_i G_i^{II}$	-25.70	-34.62	0
11018.56	g_i	0	0	11.87
	$g_i G_i^{II}$	0	0	-20.43

TABLE XXVII: The poles for Ω_{bc} along with their coupling constants (in units of MeV) to various channels in the $J^P = \frac{1}{2}^-, \frac{3}{2}^-$ sector from $VB(\frac{1}{2}^+)$.

Poles		$\Omega_{bc}\omega$	$\Xi_c\bar{B}^*$	$\Xi_b D^*$	$\Xi_{bc}\bar{K}^*$	$\Omega'_{bc}\omega$	$\Xi'_{bc}\bar{K}^*$	$\Xi'_c\bar{B}^*$	$\Xi'_b D^*$
7612.44	g_i	0	11.56	0	0	0	0	0	0
	$g_i G_i^{II}$	0	-19.93	0	0	0	0	0	0
7627.73	g_i	1.09	0	6.36	2.14	0	0	0	0
	$g_i G_i^{II}$	-9.13	0	-28.05	-15.65	0	0	0	0
7707.67	g_i	1.19	0	-2.17	3.40	0	0	0	0
	$g_i G_i^{II}$	-13.85	0	14.00	-33.94	0	0	0	0
7716.28	g_i	0	0	0	0	1.43	4.03	0	-1.77
	$g_i G_i^{II}$	0	0	0	0	-14.61	-37.19	0	6.54
7720.07	g_i	0	0	0	0	0	0	11.59	0
	$g_i G_i^{II}$	0	0	0	0	0	0	-19.97	0
7777.47	g_i	0	0	0	0	0.78	0.38	0	6.50
	$g_i G_i^{II}$	0	0	0	0	-11.04	-4.84	0	-30.09

TABLE XXVIII: The poles for Ω_{bc} along with their coupling constants (in units of MeV) to various channels in the $J^P = \frac{3}{2}^-$ sector from $PB(\frac{3}{2}^+)$.

Poles		$\Xi_{bc}^*\bar{K}$	$\Omega_{bc}^*\eta$	Ξ_b^*D	$\Xi_c^*\bar{B}$
7415.55	g_i	2.63	1.56	1.21	0
	$g_i G_i^{II}$	-40.83	-13.37	-3.05	0
7667.65 + i1.40	g_i	-0.02 - i0.20	0.02 - i0.06	6.25 - i0.05	0
	$g_i G_i^{II}$	6.82 + i0.98	0.53 + i1.88	-32.26 + i0.09	0
7740.93	g_i	0	0	0	11.52
	$g_i G_i^{II}$	0	0	0	-20.08

TABLE XXIX: The poles for Ω_{bc} along with their coupling constants (in units of MeV) to various channels in the $J^P = \frac{1}{2}^-, \frac{3}{2}^-, \frac{5}{2}^-$ sector from $VB(\frac{3}{2}^+)$.

Poles		$\Omega_{bc}^*\omega$	$\Xi_{bc}^*\bar{K}^*$	$\Xi_b^*D^*$	$\Xi_c^*\bar{B}^*$
7729.11	g_i	1.60	3.82	3.54	0
	$g_i G_i^{II}$	-15.96	-33.56	-12.92	0
7786.71	g_i	0	0	0	11.61
	$g_i G_i^{II}$	0	0	0	-19.99
7811.82	g_i	-0.23	-1.24	5.71	0
	$g_i G_i^{II}$	3.72	16.77	-28.48	0

For the case of $PB(\frac{1}{2}^+)$ states, shown in Table XXVI, we find six states coupling mostly to $\Xi_{bc}\bar{K}$, $\Xi'_c\bar{K}$, $\Xi_b D$, $\Xi_c\bar{B}$, $\Xi'_b D$, and $\Xi'_c\bar{B}$, respectively. For the case of $VB(\frac{1}{2}^+)$ we find six states, shown in Table XXVII, coupling mostly to $\Xi_c\bar{B}^*$, $\Xi_b D^*$, $\Xi_{bc}\bar{K}^*$, $\Xi'_c\bar{K}^*$, $\Xi'_c\bar{B}^*$, and $\Xi'_b D^*$, respectively.

For the case of $PB(\frac{3}{2}^+)$ with $J^P = \frac{3}{2}^-$ we show the states found in Table XXVIII. We obtain three states coupling mostly to $\Xi_{bc}^*\bar{K}$, Ξ_b^*D , and $\Xi_c^*\bar{B}$, respectively. The widths are also small, all of them below 3 MeV. For the case of $VB(\frac{3}{2}^+)$ we obtain three states of $J^P = \frac{1}{2}^-, \frac{3}{2}^-, \frac{5}{2}^-$, shown in Table XXIX, coupling mostly to $\Xi_{bc}^*\bar{K}^*$, $\Xi_c^*\bar{B}^*$, and $\Xi_b^*D^*$ respectively.

The widths obtained are small in all cases. In the cases of $VB(\frac{1}{2}^+)$, $PB(\frac{3}{2}^+)$, and $VB(\frac{3}{2}^+)$ there can be transitions to the $PB(\frac{1}{2}^+)$ states, but we anticipated that these transitions are very suppressed and the widths should be smaller than those found for transitions allowed by vector exchange within the blocks considered. For the case of $PB(\frac{1}{2}^+)$, the 4070 MeV state that couples to $\Xi_{cc}\bar{K}$ cannot decay to any other state in our space, since it is bound in $\Xi_{cc}\bar{K}$ and this channel has the smallest

threshold. The state with 4205 MeV can only decay to $\Xi_{cc}\bar{K}$, so this should be the channel to observe it. The state at 4311 MeV can decay to $\Omega_{cc}\eta$ and $\Xi_{cc}\bar{K}$. Given the couplings to the channels in Table XVIII, the favored channel for observation would be $\Omega_{cc}\eta$. Similar considerations can be done in the other sectors.

IV. ESTIMATION OF UNCERTAINTIES

As was done in Ref. [76], we estimate uncertainties in the results, as a consequence of uncertainties in the cut off, or the strength of the interaction governed by the parameter f_π . The value of q_{max} has been taken as 650 MeV, as in [76], where three experimental Ω_c states were well reproduced. Given the analogy of the states studied here, this should be a good starting point to have a realistic estimate of the states that appear from the interaction in coupled channels. However, it is also interesting to see what uncertainties we can have in the masses, widths and couplings obtained. For this we follow the same strategy as in Ref. [76] and repeat the calculations for $q_{max} = 600, 700$ MeV or $f_\pi = 97.6$ MeV (rather than 93 MeV). We also perform another sort of calculation. We position ourselves in the hypothetical situation where the experiment has been done and the states predicted are observed. A qualitative agreement with the experimental results is expected, but, as usually done, we would take one experimental mass and do fine tuning of q_{max} to get this mass. The rest of masses and widths would then be genuine predictions.

The exercise has been done for the Ω_{bc} states, where more states appear. We have checked that in the other sectors, the conclusions are the same, and for the sake of conciseness we report the results in the Ω_{bc} sector. The results are shown in Table XXX.

We observe in Table XXX that a change of 50 MeV in q_{max} reverts in changes of the masses by 10-35 MeV. In the case of the $3/2^+$ states the difference can even be bigger, up to 50 MeV. The change of f_π keeping $q_{max} = 650$ MeV induces changes of 10-20 MeV in the mass.

More interesting is to see the change when we change f_π and at the same time q_{max} in order to have the same mass of one of the states, in this case the $PB(1/2^+)$ state at 7362.26 MeV. There we find that the other masses change within the range 0-10 MeV and the widths change within 10%. The couplings to the main channel also change within 10%. This tells us the level of accuracy that we can expect once the experiments are performed, and some states are observed, and we fine tune our parameters to obtain the mass of one of the states.

TABLE XXX: The poles for Ω_{bc} with different q_{max} and f_π .

	$f_\pi = 93$ $q_{max} = 600$	$f_\pi = 93$ $q_{max} = 650$	$f_\pi = 93$ $q_{max} = 700$	$f_\pi = 97.6$ $q_{max} = 650$	$f_\pi = 97.6$ $q_{max} = 692.2$
$PB(\frac{1}{2}^+)$	7377.58	7362.26	7345.03	7374.90	7362.26
	7406.39	7392.60	7377.65	7404.44	7393.32
	$7547.32 + i1.72$	$7514.32 + i2.21$	$7477.58 + i2.58$	$7532.81 + i2.16$	$7504.85 + i2.59$
	7606.82	7566.65	7520.57	7587.93	7553.26
	$7676.65 + i2.78$	$7641.20 + i2.26$	$7601.40 + i0.95$	$7660.99 + i2.52$	$7630.80 + i2.00$
	7714.92	7674.29	7627.67	7695.67	7660.58
$VB(\frac{1}{2}^+)$	7652.65	7612.44	7566.30	7633.72	7599.01
	7665.15	7627.73	7586.28	7648.39	7616.67
	7730.21	7707.67	7682.99	7722.76	7704.10
	7742.10	7716.28	7687.80	7733.27	7711.72
	7760.74	7720.07	7673.40	7741.46	7706.33
	7811.99	7777.47	7738.99	7796.55	7767.20
$PB(\frac{3}{2}^+)$	7429.99	7415.55	7399.73	7427.74	7416.00
	$7701.15 + i0.95$	$7667.65 + i1.40$	$7630.12 + i1.83$	$7686.35 + i1.30$	$7657.87 + i1.67$
	7781.82	7740.93	7693.99	7762.36	7727.03
$VB(\frac{3}{2}^+)$	7758.72	7729.11	7695.70	7747.68	7722.48
	7827.64	7786.71	7739.72	7808.15	7772.78
	7842.05	7811.82	7779.12	7828.91	7803.79

V. CONCLUSION

We have done a thorough study of the molecular states of type $\Omega_{cc}, \Omega_{bb}, \Omega_{bc}$ that stem from the interaction of meson baryon coupled channels with these quantum numbers. We classify them as $PB(\frac{1}{2}^+), PB(\frac{3}{2}^+), VB(\frac{1}{2}^+), VB(\frac{3}{2}^+)$, hence, channels

composed of a meson, pseudoscalar or vector, and a baryon in its ground state with either spin $\frac{1}{2}$ or $\frac{3}{2}$. The interaction is evaluated using an extension of the local hidden gauge approach and we only consider S -wave. Hence we obtain states carrying $J^P = \frac{1}{2}^-, \frac{3}{2}^-, \frac{5}{2}^-$. In the case of $VB(\frac{1}{2}^+)$ we have degenerate states in $J^P = \frac{1}{2}^-, \frac{3}{2}^-$ and in the case of $VB(\frac{3}{2}^+)$ we obtain degenerate states with $J^P = \frac{1}{2}^-, \frac{3}{2}^-, \frac{5}{2}^-$. We obtain states of each type for the three $\Omega_{cc}, \Omega_{bb}, \Omega_{bc}$ sectors. We look for poles of the scattering matrix in the second Riemann sheet and then evaluate the couplings of the states obtained to each channel. Simultaneously, we also evaluate the wave function at the origin. In all the states observed we find one channel that has a much bigger coupling and wave function at the origin than the other channels, which we identify as the main component of the wave function of that state in terms of the coupled channels considered. Although in the case of coupled channels it is difficult to define a binding, if we refer to the threshold of the main component, we find bindings of the order of 50-130 MeV. These bindings are in the line of bindings obtained for other case as Ω_c, Ξ_c, Ξ_b etc., whose agreement with some states found experimentally has been reported.

The states that we have chosen to study here are presently under analysis by the LHCb collaboration and it will be most instructive to compare with the experimental results whenever they are available.

VI. ACKNOWLEDGEMENT

W. F. Wang and J. Song thank Meng-Lin Du for valuable discussions. J. Song also wishes to acknowledge support from China Scholarship Council. This work was supported in part by the National Natural Science Foundation of China under Grant No. 12147215. This work was partly supported by the Spanish Ministerio de Economía y Competitividad (MINECO) and 16 European FEDER funds under Contracts No. PID2020-112777GB-I00, and by Generalitat Valenciana under contract PROMETEO/2020/023. This project has received funding from the European Union Horizon 2020 research and innovation programme under the program H2020-INFRAIA-2018-1, grant agreement No. 824093 of the STRONG-2020 project. The work of A. F. was partially supported by the Generalitat Valenciana and European Social Fund APOSTD-2021-112.

-
- [1] K. W. Edwards et al. (CLEO), Phys. Rev. Lett. **74**, 3331 (1995).
 - [2] H. Albrecht et al. (ARGUS), Phys. Lett. B **317**, 227 (1993).
 - [3] M. Artuso et al. (CLEO), Phys. Rev. Lett. **86**, 4479 (2001), hep-ex/0010080.
 - [4] R. Aaij et al. (LHCb), JHEP **05**, 030 (2017), 1701.07873.
 - [5] B. Aubert et al. (BaBar), Phys. Rev. Lett. **98**, 012001 (2007), hep-ex/0603052.
 - [6] R. Mizuk et al. (Belle), Phys. Rev. Lett. **94**, 122002 (2005), hep-ex/0412069.
 - [7] S. E. Csorna et al. (CLEO), Phys. Rev. Lett. **86**, 4243 (2001), hep-ex/0012020.
 - [8] J. P. Alexander et al. (CLEO), Phys. Rev. Lett. **83**, 3390 (1999), hep-ex/9906013.
 - [9] B. Aubert et al. (BaBar), Phys. Rev. D **77**, 031101 (2008), 0710.5775.
 - [10] R. Aaij et al. (LHCb), Phys. Rev. Lett. **124**, 222001 (2020), 2003.13649.
 - [11] R. Chistov et al. (Belle), Phys. Rev. Lett. **97**, 162001 (2006), hep-ex/0606051.
 - [12] T. J. Moon et al. (Belle), Phys. Rev. D **103**, L111101 (2021), 2007.14700.
 - [13] B. Aubert et al. (BaBar), Phys. Rev. D **77**, 012002 (2008), 0710.5763.
 - [14] R. Aaij et al. (LHCb), Phys. Rev. Lett. **118**, 182001 (2017), 1703.04639.
 - [15] R. Aaij et al. (LHCb), Phys. Rev. Lett. **109**, 172003 (2012), 1205.3452.
 - [16] T. A. Aaltonen et al. (CDF), Phys. Rev. D **88**, 071101 (2013), 1308.1760.
 - [17] A. M. Sirunyan et al. (CMS), Phys. Lett. B **803**, 135345 (2020), 2001.06533.
 - [18] R. Aaij et al. (LHCb), JHEP **06**, 136 (2020), 2002.05112.
 - [19] R. Aaij et al. (LHCb), Phys. Rev. Lett. **123**, 152001 (2019), 1907.13598.
 - [20] R. Aaij et al. (LHCb), Phys. Rev. Lett. **122**, 012001 (2019), 1809.07752.
 - [21] A. M. Sirunyan et al. (CMS), Phys. Rev. Lett. **126**, 252003 (2021), 2102.04524.
 - [22] R. Aaij et al. (LHCb), Phys. Rev. Lett. **121**, 072002 (2018), 1805.09418.
 - [23] R. Aaij et al. (LHCb), Phys. Rev. D **103**, 012004 (2021), 2010.14485.
 - [24] R. Aaij et al. (LHCb), Phys. Rev. Lett. **128**, 162001 (2022), 2110.04497.
 - [25] R. Aaij et al. (LHCb), Phys. Rev. Lett. **124**, 082002 (2020), 2001.00851.
 - [26] H.-X. Chen, W. Chen, X. Liu, Y.-R. Liu, and S.-L. Zhu (2022), 2204.02649.
 - [27] R. Aaij et al. (LHCb), Phys. Rev. Lett. **115**, 072001 (2015), 1507.03414.
 - [28] R. Aaij et al. (LHCb), Phys. Rev. Lett. **122**, 222001 (2019), 1904.03947.
 - [29] R. Aaij et al. (LHCb), Phys. Rev. Lett. **128**, 062001 (2022), 2108.04720.
 - [30] R. Aaij et al. (LHCb), Sci. Bull. **66**, 1278 (2021), 2012.10380.
 - [31] R. Aaij et al. (LHCb), Chin. Phys. C **45**, 093002 (2021), 2104.04759.
 - [32] S. S. Gershtein, V. V. Kiselev, A. K. Likhoded, and A. I. Onishchenko, Mod. Phys. Lett. A **14**, 135 (1999), hep-ph/9807375.
 - [33] S. S. Gershtein, V. V. Kiselev, A. K. Likhoded, and A. I. Onishchenko, Phys. Rev. D **62**, 054021 (2000).

- [34] D. Ebert, R. N. Faustov, V. O. Galkin, and A. P. Martynenko, *Phys. Rev. D* **66**, 014008 (2002), hep-ph/0201217.
- [35] V. V. Kiselev, A. K. Likhoded, O. N. Pakhomova, and V. A. Saleev, *Phys. Rev. D* **66**, 034030 (2002), hep-ph/0206140.
- [36] W. Roberts and M. Pervin, *Int. J. Mod. Phys. A* **23**, 2817 (2008), 0711.2492.
- [37] A. Valcarce, H. Garcilazo, and J. Vijande, *Eur. Phys. J. A* **37**, 217 (2008), 0807.2973.
- [38] C. Albertus, E. Hernandez, and J. Nieves, *Phys. Lett. B* **683**, 21 (2010), 0911.0889.
- [39] C. Albertus, E. Hernandez, and J. Nieves, *Phys. Rev. D* **85**, 094035 (2012), 1202.4861.
- [40] Y.-L. Ma and M. Harada, *Phys. Lett. B* **748**, 463 (2015), 1503.05373.
- [41] Z. Shah, K. Thakkar, and A. K. Rai, *Eur. Phys. J. C* **76**, 530 (2016), 1609.03030.
- [42] H. Garcilazo, A. Valcarce, and J. Vijande, *Phys. Rev. D* **94**, 074003 (2016), 1609.06886.
- [43] Q.-F. Lü, K.-L. Wang, L.-Y. Xiao, and X.-H. Zhong, *Phys. Rev. D* **96**, 114006 (2017), 1708.04468.
- [44] L.-Y. Xiao, Q.-F. Lü, and S.-L. Zhu, *Phys. Rev. D* **97**, 074005 (2018), 1712.07295.
- [45] J.-J. Niu, L. Guo, H.-H. Ma, X.-G. Wu, and X.-C. Zheng, *Phys. Rev. D* **98**, 094021 (2018), 1810.03834.
- [46] N. Salehi and N. Mohajery, *Eur. Phys. J. Plus* **133**, 416 (2018).
- [47] Q. Li, C.-H. Chang, S.-X. Qin, and G.-L. Wang, *Chin. Phys. C* **44**, 013102 (2020), 1903.02282.
- [48] L. X. Gutiérrez-Guerrero, A. Bashir, M. A. Bedolla, and E. Santopinto, *Phys. Rev. D* **100**, 114032 (2019), 1911.09213.
- [49] Z. Shah, A. Kakadiya, K. Gandhi, and A. K. Rai, *Universe* **7**, 337 (2021).
- [50] Z. Ghalenovi, C.-P. Shen, and M. M. Sorkhi (2022), 2204.02938.
- [51] R. Lewis, N. Mathur, and R. M. Woloshyn, *Phys. Rev. D* **64**, 094509 (2001), hep-ph/0107037.
- [52] H.-W. Lin, *Chin. J. Phys.* **49**, 827 (2011), 1106.1608.
- [53] Z. S. Brown, W. Detmold, S. Meinel, and K. Orginos, *Phys. Rev. D* **90**, 094507 (2014), 1409.0497.
- [54] P. Pérez-Rubio, S. Collins, and G. S. Bali, *Phys. Rev. D* **92**, 034504 (2015), 1503.08440.
- [55] H. Bahtiyar, K. U. Can, G. Erkol, M. Oka, and T. T. Takahashi, *Phys. Rev. D* **98**, 114505 (2018), 1807.06795.
- [56] R. A. Briceño, H.-W. Lin, and D. R. Bolton, *Phys. Rev. D* **86**, 094504 (2012), 1207.3536.
- [57] Z.-G. Wang, *Eur. Phys. J. A* **45**, 267 (2010), 1001.4693.
- [58] X.-H. Hu, Y.-L. Shen, W. Wang, and Z.-X. Zhao, *Chin. Phys. C* **42**, 123102 (2018), 1711.10289.
- [59] Z.-G. Wang, *Eur. Phys. J. C* **78**, 826 (2018), 1808.09820.
- [60] M. H. Weng, X. H. Guo, and A. W. Thomas, *Phys. Rev. D* **83**, 056006 (2011), 1012.0082.
- [61] M. Karliner and J. L. Rosner, *Phys. Rev. Lett.* **115**, 122001 (2015), 1506.06386.
- [62] J. Soto and J. Tarrús Castellà, *Phys. Rev. D* **102**, 014013 (2020), [Erratum: *Phys.Rev.D* 104, 059901 (2021)], 2005.00551.
- [63] J. Soto and J. Tarrús Castellà, *Phys. Rev. D* **104**, 074027 (2021), 2108.00496.
- [64] X.-K. Dong, F.-K. Guo, and B.-S. Zou, *Commun. Theor. Phys.* **73**, 125201 (2021), 2108.02673.
- [65] X.-K. Dong, F.-K. Guo, and B.-S. Zou, *Progr. Phys.* **41**, 65 (2021), 2101.01021.
- [66] X.-K. Dong, F.-K. Guo, and B. S. Zou, *Few Body Syst.* **62**, 61 (2021).
- [67] J. A. Oller, E. Oset, and A. Ramos, *Prog. Part. Nucl. Phys.* **45**, 157 (2000), hep-ph/0002193.
- [68] F.-K. Guo, C. Hanhart, U.-G. Meißner, Q. Wang, Q. Zhao, and B.-S. Zou, *Rev. Mod. Phys.* **90**, 015004 (2018), [Erratum: *Rev.Mod.Phys.* 94, 029901 (2022)], 1705.00141.
- [69] J. Hofmann and M. F. M. Lutz, *Nucl. Phys. A* **763**, 90 (2005), hep-ph/0507071.
- [70] T. Mizutani and A. Ramos, *Phys. Rev. C* **74**, 065201 (2006), hep-ph/0607257.
- [71] L. Tolos, A. Ramos, and T. Mizutani, *Phys. Rev. C* **77**, 015207 (2008), 0710.2684.
- [72] C. Garcia-Recio, V. K. Magas, T. Mizutani, J. Nieves, A. Ramos, L. L. Salcedo, and L. Tolos, *Phys. Rev. D* **79**, 054004 (2009), 0807.2969.
- [73] C. E. Jimenez-Tejero, A. Ramos, and I. Vidana, *Phys. Rev. C* **80**, 055206 (2009), 0907.5316.
- [74] O. Romanets, L. Tolos, C. Garcia-Recio, J. Nieves, L. L. Salcedo, and R. G. E. Timmermans, *Phys. Rev. D* **85**, 114032 (2012), 1202.2239.
- [75] G. Montaña, A. Feijoo, and A. Ramos, *Eur. Phys. J. A* **54**, 64 (2018), 1709.08737.
- [76] V. R. Debastiani, J. M. Dias, W. H. Liang, and E. Oset, *Phys. Rev. D* **97**, 094035 (2018), 1710.04231.
- [77] M. Bando, T. Kugo, S. Uehara, K. Yamawaki, and T. Yanagida, *Phys. Rev. Lett.* **54**, 1215 (1985).
- [78] M. Bando, T. Kugo, and K. Yamawaki, *Physics Reports* **164**, 217 (1988).
- [79] M. Harada and K. Yamawaki, *Phys. Rept.* **381**, 1 (2003), hep-ph/0302103.
- [80] U. G. Meissner, *Phys. Rept.* **161**, 213 (1988).
- [81] H. Nagahiro, L. Roca, A. Hosaka, and E. Oset, *Phys. Rev. D* **79**, 014015 (2009), 0809.0943.
- [82] J. M. Dias, V. R. Debastiani, J. J. Xie, and E. Oset, *Phys. Rev. D* **98**, 094017 (2018), 1805.03286.
- [83] J. M. Dias, Q.-X. Yu, W.-H. Liang, Z.-F. Sun, J.-J. Xie, and E. Oset, *Chin. Phys. C* **44**, 064101 (2020), 1912.04517.
- [84] Q. X. Yu, R. Pavao, V. R. Debastiani, and E. Oset, *Eur. Phys. J. C* **79**, 167 (2019), 1811.11738.
- [85] Q.-X. Yu, J. M. Dias, W.-H. Liang, and E. Oset, *Eur. Phys. J. C* **79**, 1025 (2019), 1909.13449.
- [86] W.-H. Liang, J. M. Dias, V. R. Debastiani, and E. Oset, *Nucl. Phys. B* **930**, 524 (2018), 1711.10623.
- [87] W.-H. Liang and E. Oset, *Phys. Rev. D* **101**, 054033 (2020), 2001.02929.
- [88] Y. Shimizu and M. Harada, *Phys. Rev. D* **96**, 094012 (2017), 1708.04743.
- [89] F.-K. Guo, C. Hidalgo-Duque, J. Nieves, and M. P. Valderrama, *Phys. Rev. D* **88**, 054014 (2013), 1305.4052.
- [90] R. Chen, A. Hosaka, and X. Liu, *Phys. Rev. D* **97**, 036016 (2018), 1711.07650.
- [91] C. Garcia-Recio, J. Nieves, O. Romanets, L. L. Salcedo, and L. Tolos, *Phys. Rev. D* **87**, 074034 (2013), 1302.6938.
- [92] C. Garcia-Recio, J. Nieves, O. Romanets, L. L. Salcedo, and L. Tolos, *Phys. Rev. D* **87**, 034032 (2013), 1210.4755.
- [93] J. Nieves, R. Pavao, and L. Tolos, *Eur. Phys. J. C* **80**, 22 (2020), 1911.06089.
- [94] H.-X. Chen, W. Chen, X. Liu, and S.-L. Zhu, *Phys. Rept.* **639**, 1 (2016), 1601.02092.

- [95] Y. Dong, A. Faessler, and V. E. Lyubovitskij, *Prog. Part. Nucl. Phys.* **94**, 282 (2017).
- [96] Y.-R. Liu, H.-X. Chen, W. Chen, X. Liu, and S.-L. Zhu, *Prog. Part. Nucl. Phys.* **107**, 237 (2019), 1903.11976.
- [97] A. Ramos, A. Feijoo, Q. Llorens, and G. Montaña, *Few Body Syst.* **61**, 34 (2020), 2009.04367.
- [98] S.-Y. Kong, J.-T. Zhu, D. Song, and J. He, *Phys. Rev. D* **104**, 094012 (2021), 2106.07272.
- [99] J. M. Dias, G. Toledo, L. Roca, and E. Oset, *Phys. Rev. D* **103**, 116019 (2021), 2102.08402.
- [100] J.-J. Wu, R. Molina, E. Oset, and B. S. Zou, *Phys. Rev. Lett.* **105**, 232001 (2010), 1007.0573.
- [101] C. W. Xiao, J. Nieves, and E. Oset, *Phys. Rev. D* **88**, 056012 (2013), 1304.5368.
- [102] M.-J. Yan, X.-H. Liu, S. González-Solís, F.-K. Guo, C. Hanhart, U.-G. Meißner, and B.-S. Zou, *Phys. Rev. D* **98**, 091502 (2018), 1805.10972.
- [103] N. Yalikul, Y.-H. Lin, F.-K. Guo, Y. Kamiya, and B.-S. Zou, *Phys. Rev. D* **104**, 094039 (2021), 2109.03504.
- [104] Z.-L. Wang, C.-W. Shen, D. Rönchen, U.-G. Meißner, and B.-S. Zou, *Eur. Phys. J. C* **82**, 497 (2022), 2204.12122.
- [105] S. Sakai, L. Roca, and E. Oset, *Phys. Rev. D* **96**, 054023 (2017), 1704.02196.
- [106] A. Manohar and H. Georgi, *Nucl. Phys. B* **234**, 189 (1984).
- [107] D. Gamermann, J. Nieves, E. Oset, and E. Ruiz Arriola, *Phys. Rev. D* **81**, 014029 (2010), 0911.4407.
- [108] P. A. Zyla et al. (Particle Data Group), *PTEP* **2020**, 083C01 (2020).
- [109] Q.-S. Zhou, K. Chen, X. Liu, Y.-R. Liu, and S.-L. Zhu, *Phys. Rev. C* **98**, 045204 (2018), 1801.04557.